

南京航空航天大学  
论文集

(二〇一〇年) 第21册

电子信息工程学院

(第2分册)

南京航空航天大学科技部编

二〇一一年五月



NUAA2011039778

Z427  
1033(2010)-(21)

# 电子信息工程学院

041~042



2011039778

21

电子信息工程学院2010年发表论文目录

序号	姓名	单位	职称	论文题目	刊物、会议名称	发表时间	类别
74	邓宏 伟永 赵久 张璐	041 042 042 042 041	博 士 教 授 硕 士 硕 士 博 士	Quadruple-Mode Stub-Loaded Resonator and Broadband BPF	Progress in Electromagnetics Research Letters	2010年18卷	
75	邓宏 伟永 赵久 张学	041 042 042 042 042	博 士 教 授 硕 士 硕 士 博 士	High Selectivity Broadband Bandpass Filter with Dual-Mode folded-T-type resonator	Progress in Electromagnetics Research Letters	2010年19卷	
76	潘时 龙	041	正 高	Transient state of wavelength tuning in mode-locked laser with a dispersive cavity	Asia Communications & Photonics Conference & Exhibition (ACP 2010)	2010	
77	毛飞 吴宁	041 041	博 士 教 授	伪随机屏蔽二进序列码	系统工程与电子技术	2010年32卷3期	
78	万玉 鹏	041 041	硕 士 教 授	基于自适应算法的NoC路由单元的系统级设计	微电子学与计算机	2010年27卷5期	
79	刘静 吴	041 041 041	硕 士 教 授 硕 士	嵌入式图形处理器中几何变换引擎的设计	计算机仿真	2010年27卷1期	
80	丁昌 圣吴 宁	041 041 041	硕 士 教 授 讲 师	基于PX27x的摄像头系统的设计与实现	南京师范大学学报	2010年10卷4期	
81	高松	041 041	硕 士 教 授	基于TeeChart的热流分析系统设计	工业控制计算机	2010年23卷9期	
82	王疏	041 041	硕 士 教 授	PXA270的电池充电及电量计量模块设计	单片机与嵌入式系统应用	2010年27卷9期	
83	罗丹	041 041	硕 士 教 授	基于OCP接口的片上网络性能评估平台	中国集成电路	2010年19卷8期	
84	张京 陵牛 臻	041 041	硕 士 副 教授	Simulation of Electromagnetic Interference from GSM Wireless Phones in transport Airplanes	ISAPE 2010	2010	
85	刘云 牛臻 弋	041 041 041	硕 士 副 教授 硕 士	DUAL-BAND H-SHAPED SLOT ANTENNA FOR 2.4 AND 5GHz WIRELESS COMMUNICATION	MICROWAVE AND OPTICAL TECHNOLOGY LETTERS	2010年4卷52期	
86	葛芬 吴	041 041	中 级 教 授	Genetic Algorithm Based Mapping and Routing Approach for Network on Chip Architectures	Chinese Journal of Electronics	2010年19卷1期	
87	葛芬 吴	041 041	中 级 教 授	面向特定应用的片上网络低能耗拓扑生成方法	系统工程与电子技术	2010年32卷8期	
88	葛芬 吴宁	041 041	中 级 教 授	Simulation and Performance Analysis of Network on Chip Architectures	Transactions of Nanjing University of Aeronautics & Astronautics	2010年27卷4期	
89	唐金 华邵	041 041	硕 士 高 工	基于BP神经网络的任意副频响应FIR滤波器的设计	第7届中国通信学会学术年会论文集	2010	
90	容亦 夏邵	041 041	硕 士 高 工	基于三次样条曲面的多波束测深信息处理	计算机技术与发展	2010年20卷2期	
91	邵	041	副 高	基于SVM的多波束测深数据滤波	CCC2010 Proceeding	2010	
92	邵	041	副 高	基于质点引力模型的中值滤波算法	CCC2010 Proceeding	2010	



93	龙伟军 Asim D B	042 042 042	博 士 教 授 副 教 授	三维机会阵雷达波速综合优化	电波科学学报	2010年25卷1期	
94	陶满意 李勇岱 朱 寅	042 042 042	硕 士 副 教 授 教 授	Signal Based Parameter Estimation for Precise Circular-scanning SAR Imaging	Proceedings of International Symposium on Signal, Systems and Electronics (ISSSE2010)	2010. 9	
95	王娟娟 李勇化 段 化	042 042 042	硕 士 副 教 授 硕 士	改进的机动航迹聚束SAR运动补偿算法研究	第十一届全国雷达学术年会论文集	2010. 11	
96	段 化 军 勇 李 勇	042 042 042	硕 士 副 教 授 硕 士	一种改进的气象雷达降水回波与地杂波建模和仿真方法	第十一届全国雷达学术年会论文集	2010. 11	
97	李勇岱 朱 寅	042 042	副 教 授 教 授	The Geometric-distortion Correction Algorithm for Circular-scanning SAR Imaging	IEEE Geoscience and remote sensing letters	2010年7卷2期	
98	金雪松	042 042	硕 士 副 教 授	环视SAR双条带成像实现方案	遥感学报	2010年14卷4期	
99	金雪松 李 勇	042 042	硕 士 副 教 授	Implementation of dual stripmap imaging for a novel airborne SAR system	遥感学报	2010年14卷4期	
100	薛小龙 雷磊	042 042 042	硕 士 讲 师 教 授	硬件平台上的HEED实现及其性能分析	计算机工程	2010年36卷13期	
101	朱颖峰 雷磊	042 042 042	硕 士 讲 师 教 授	基于综合度量Ad hoc网络跨层路由协议	计算机工程	2010年36卷18期	
102	方理才 雷磊	042 042 042	硕 士 讲 师 教 授	基于节点合作的Ad hoc网多信道MAC协议	计算机工程	2010年36卷18期	
103	杜业珍 雷磊	042 042 042	硕 士 讲 师 教 授	WiMAX系统突发实时业务调度算法的改进	计算机工程	2010年36卷21期	
104	雷磊 徐宗	042 042	中 级 教 授	Ad hoc网络中信号干扰对DCF协议公平性的影响及仿真分析	系统仿真学报	2010年22卷1期	
105	雷磊 朱青	042 042	中 级 硕 士	Analyzing and Improving the Simulation Algorithm of IEEE 802.11 DCF Error Frame Model in QualNet Simulator	International Conference on Multimedia Information Networking and Security	2010	
106	雷磊 田加敏	042 042	中 级 硕 士	A Mechanism Based on Node Cooperation for Improving DCF 0/1 Fairness in Ad hoc Networks	International Conference on Internet Technology and Applications , ITAP 2010	2010	
107	雷磊 薛小	042 042	中 级 硕 士	实现节点负载均衡的无线传感网能量高效分簇方法	应用科学学报	2010年28卷6期	
108	雷磊 徐宗	042 042	中 级 教 授	基于定长时隙的多跳Ad Hoc网络DCF协议马尔可夫链模型	软件学报	2010年21卷3期	
109	王旭	042	中 级	基于STFT的宽带数字ESM接收技术	系统工程与电子技术	2010年32卷9期	
110	王旭东	042	中 级	Adaptive Radar Pulse Deinterleaving Method Based on Auto-associative Artificial Neural Network	Power and Energy Engineering Conference (PEEC 2010)	2010	
111	王旭东	042	中 级	Joint Angle and Frequency Estimation Using Multiple-Delay Output Based on ESPRIT	EURASIP Journal on Advances in Signal Processing	2010. 12	

112	王旭东	042	中 级	无监督Eidos表相盒中脑状态人工神经网络模型参数优化选取	控制理论与应用	2010年27卷3期	
113	王旭东	042	中 级	基于Eidos BSB人工神经网络的雷达脉冲分选方法	现代电子技术	2010年34卷23期	
114	王劲宋茂	042 042	硕 士 教 授	GPS软件接收机弱信号捕获系统设计	武汉大学学报（信息科学版）	2010年35卷7期	
115	宋晓宋茂	042 042	硕 士 教 授	时空调制MT-CDMA多目标通信测控系统	苏州科技学院学报（自然科学版）	2010年1期	
116	金校江	042 042	硕 士 教 授	混合二进制偏移载波调制信号快捕算法设计	苏州科技学院学报（工程技术版）	2010年1期	
117	崔海逢	042 042	硕 士 教 授	基于FPGA的GPS信号采集及网络传输	江南大学学报（自然科学版）	2010年9卷1期	
118	陈守强	042 042	硕 士 教 授	基于分段相关的GPS快速捕获系统设计	电子信息对抗技术	2010年5期	
119	汪飞葛琦周建江	042 042 042	副教授 硕 士 教 授	Scattering Centers Extraction of Radar Target Using Biquaternions	International Conference on Measuring Technology and Mechatronics Automation	2010	
120	汪飞李海林	042 042 042	副教授 讲 师 教 授	Joint multiple parameters estimation for vector-sensor array using biquaternions	ICIC Express Letters	2010年4卷5B期	
121	汪 玲	042	副 高	Passive imaging using distributed apertures in multiple-scattering environments	Inverse Problems	2010	
122	汪 玲	042	副 高	Passive imaging exploiting multiple scattering using distributed apertures	Proceedings of 2010 IEEE International Conference on Image Processing (ICIP 2010)	2010	
123	汪 玲	042	副 高	Passive radar imaging of moving targets with sparsely distributed receivers	The 6 <sup>th</sup> IEEE Sensor Array and Multichannel Signal Processing Workshop (SAM 2010)	2010	
124	汪 玲	042	副 高	Passive Doppler synthetic aperture radar imaging	EUSAR 2010 Proceedings	2010	
125	汪玲叶旭朱岱寅	042 042 042 042	副 高 硕 士 教 授 教 授	Novel side-view imaging of ships at sea for airborne ISAR	2010 IEEE International Radar Conference Proceedings	2010	
126	汪 玲	042	副 高	Doppler synthetic aperture hitchhiker imaging	Proceedings of SPIE on Defense, Security and Sensing 2010	2010	
127	汪 玲	042	副 高	Multistatic Radar Imaging of Moving Targets	2010 IEEE International Radar Conference Proceedings	2010	
128	刘冬张弓	042 042	硕 士 教 授	基于指数小波分形特征的SAR图像特定目标检验	西安电子科技大学学报	2010年37卷2期	
129	宛书成张弓	042 042 042	硕 士 教 授 硕 士	打击效果仿真研究	计算机应用研究	2010年27卷7期	
130	何永丛张弓	033 042 042	硕 士 教 授 教 授	基于半变异函数及不变矩的SAR图像检索	光电工程	2010年37卷3期	
131	刘帅张弓刘文	033 042 042	硕 士 教 授 教 授	基于时空结构的双基MIMO雷达多维参数联合估计	航空学报	2010年31卷6期	

132	翟伟伟 张弓	033 042 042	硕 士 教 授 教 授	基于杂波子空间估计的MIMO雷达降维STAP研究	航空学报	2010年31卷9期	
133	施张刘 张群文	033 042 042	硕 士 教 授 教 授	混沌理论在MIMO雷达波形设计中的应用	数据采集与处理	2010年25卷4期	
134	毛新	042	中 级	匀速运动目标的聚束SAR成像特征分析	数据采集与处理	2010年25卷3期	
135	毛新华	042	中 级	一种基于图像后处理的极坐标格式算法波前弯曲补偿方法	电子学报	2010年38卷1期	
136	毛新华	042	中 级	Comparative study of rma and pfa on their responses to moving target	Progress In Electromagnetics Research	2010年110期	
137	胥嘉佳 刘渝刚	042 042 042	博 士 教 授 博 士	两ADC异步采样信号频率无模糊估计算法	数据采集与处理	2010. 10. 15	
138	胡国兵 刘渝刚 邓振森	042 042 042 042	博 士 教 授 博 士 博 士	复杂体制脉冲重复间隔调制方式识别	数据采集与处理	2010. 10. 15	
139	张刚兵 刘渝刚 胥嘉	042 042 042	博 士 教 授 博 士	基于UKF的单站无源定位与跟踪双向预测滤波算法	系统工程与电子技术	2010. 7. 15	
140	张刚兵 刘渝刚 邓振	042 042 042	博 士 教 授 博 士	相参脉冲串多普勒频率变化率估计算法	数据采集与处理	2010. 9. 15	
141	魏敏黎 黎宁	042 042	硕 士 副 教授	高斯核尺寸对SIFT算法的影响	第四届（CTC2010）全国通信新理论与新技术学术大会	2010	
142	张文娜	042 042	硕 士 副 教授	基于蓝牙跳频原理的通信系统仿真	福建电脑	2010年8期	
143	王昕朱 朱岱寅 朱兆	042 042 042	博 士 教 授 教 授	An Implementation of Bistatic PFA Using Chirp Scaling	Journal of Electromagnetic Waves and Application	2010年24卷4-5期	
144	王昕朱 朱岱寅	042 042	博 士 教 授	Wavefront Curvature Correction in One Stationary Bistatic SAR Image Focused via PFA	IET Electronics Letters	2010年46卷18期	
145	田斌朱 朱岱寅 朱兆	042 042 042	博 士 教 授 教 授	利用样本协方差矩阵特征分解实现双通道SAR动目标检测	电子与信息学报	2010年32卷11期	
146	田斌朱 朱岱寅 朱兆	042 042 042	博 士 教 授 教 授	An Improved SAR-GMTI Method based on Eigen-Decomposition of the Sample Covariance Matrix	Journal of Electronics (China)	2010年3卷27期	
147	蒋锐朱 朱岱寅 朱兆	042 042 042	博 士 教 授 教 授	一种用于条带模式SAR成像的自聚焦算法	航空学报	2010年31卷12期	
148	吴迪朱 朱岱寅 朱兆	042 042 042	博 士 教 授 教 授	机载雷达单脉冲前视成像算法	中国图像图形学报	2010, 15 (3)	
149	吴迪朱 朱岱寅 朱兆	042 042 042	博 士 教 授 教 授	基于改进FRACTA算法的多通道SAR动目标检测技术	电子与信息学报	2010, 32 (9)	

150	吴迪 朱岱寅 朱兆	042 042 042	博 教 教	士 授 授	一种非均匀环境中双端口干涉 SAR/GMTI杂波抑制算法	电子学报	2010, 15 (3)	
151	吴迪 朱岱寅 朱兆	042 042 042	博 教 教	士 授 授	Knowledge-Aided Multichannel Adaptive SAR/GMTI Processing:Algorithm and Experimental Results	EURASIP Journal on Advances in Signal Processing	2010	
152	朱岱寅 毛新华 李勇	042 042 042 042	教 讲 副 教	授 师 教 授	Far-Field Limit of PFA for SAR Moving Target Imaging	IEEE Transactions on Aerospace and Electronic Systems	2010年46卷2期	
153	李俊 平 胡文 赵广	042 042 042	硕 中 硕	士 级 士	线性自调频系统	中国电子学会电路与 系统学会第二十二届 年会	2010年10月	
154	胡文伯 包成 张弓 刘贤 龙	042 042 042 042 042	中 正 正 正 中	级 高 高 高 高级	基于混沌同步的线性卷积系统辨识	东南大学学报	2010年40卷6期	
155	虞湘 宾	042	副	高	Performance of a Space-time Block Coded Code Division Multiple Access System over Nakagami-m Fading Channels	Internation Journal of Electronics	2010年97卷9期	
156	虞湘 宾	042	副	高	Performance of Multiband Complex- Wavelet-Based MC-CDMA System with Space-Time Coding over Nakagami-m Fading Channels	Circuits, Systems and Signal Processing	2010年29卷3期	
157	虞湘 宾	042	副	高	Performance Analysis of Variable- power Adaptive Modulation in Space-time Block Coded MIMO Diversity Systems	SCIENCE CHINA Information Sciences	2010年53卷10 期	
158	虞湘 宾	042	副	高	Performance Analysis of Discrete- Rate Adaptive Modulation with Space-Time Coding in Multiple Antennas System	Second International Conference on Networks Security Wireless Communications and Trusted Computing(NSWCTC' 20 10)	2010	
159	虞湘 宾	042	副	高	Receiver Design for Multiuser CDMA Systems with Space-time Coding and Imperfect State Information	Second International Conference on Communication Systems, Networks and Applications(ICCNSA '2010)	2010	
160	陈未 央 孙中 伟	042 042 042	硕 硕 教	士 士 授	Multi-invariance MUSIC algorithm for DOA estimation in acoustic vector-sensor Array	CCCM2010	2010年1卷	
161	张小 飞 冯高 鹏	042 042 042 042	正 硕 硕 教	高 士 士 授	Blind multiuser detection for MC- CDMA with antenna array	Computers and Electrical Engineering	2010年36卷1期	

## QUADRUPLE-MODE STUB-LOADED RESONATOR AND BROADBAND BPF

H.-W. Deng, Y.-J. Zhao, L. Zhang, X.-S. Zhang, and W. Zhao

College of Information Science and Technology  
Nanjing University of Aeronautics and Astronautics  
Nanjing, China

**Abstract**—Novel compact microstrip quadruple-mode stub-loaded resonator and broadband bandpass filter (BPF) are proposed in this letter. As a starting part of designing a quadruple-mode broadband BPF, the initial novel triple-mode open impedance-stepped stub loaded resonator characteristic is investigated to choose its proper dimensions. Based on these pre-determined dimensions of the triple-mode resonator, two identical short-circuited stubs are loaded against the impedance-stepped open stubs in the resonator to generate a tuned resonant mode and a transmission zero in lower stopband which leads to a high rejection skirt. A compact broadband BPF with the quadruple-mode resonator is simulated, fabricated and measured. The measured results agree well with the EM simulations.

### 1. INTRODUCTION

Recently, compact size, wide stopband and high selectivity microwave BPFs are widely applied to enhance the performance of radio frequency (RF) front-ends. Resonators, as the fundamental elements in a filter, usually determine the size of the filter. There are many ways to reduce the resonator size, however, the important way for the filter size reduction is to modify the traditional resonator to generate additional modes, causing the resonator to have multiple resonate frequencies and thus one physical resonator can be treated as multiple electrical resonators. Examples can be seen from dual-mode ring resonator [1], dual-mode square-ring resonator [2] and dual-mode

---

*Received 17 June 2010, Accepted 20 September 2010, Scheduled 24 September 2010*  
Corresponding author: H.-W. Deng (ceceliayan1008@yahoo.com.cn).



multi-arc resonator [3]. The dual-mode means two degenerate resonant modes of the aforementioned geometrically symmetrical resonators and the two degenerate resonant modes may be split by introducing a perturbation element in a resonator. Subsequently, the dual-mode resonator that odd and even modes do not couple has been given in [4]. Some triple-mode resonators [5,6] have been presented to design BPFs with high frequency selectivity. However, the fractional bandwidths of the BPFs are less than 5%. Recently, several BPFs with the fractional bandwidth better than 110% are reported using the triple-mode impedance-stepped resonators (SIR), such as stub-loaded multiple-mode resonator (MMR) [7], EBG-embedded MMR [8], one open stub and one short stub loaded MMR [9]. Then, a quadruple-mode SIR by Wong and Zhu [10] is proposed to build up UWB filter with compact size. In [11], instead of using multimode SIR, a dual-mode resonator composed of single stub at the center plane and two sections of transmission lines is introduced for high rejection and wideband BPF with the fractional bandwidth 45%.

The primary objective of this work is to explore a compact high selectivity and broadband BPF with quadruple-mode resonator. As part of the designing quadruple-mode filter, an initial novel compact triple-mode open impedance-stepped stub loaded resonator is firstly constituted in Section 2. Then, two identical short-circuited stubs are properly attached to the triple-mode resonator to form a quadruple-mode resonator in Section 3. After the principle of the quadruple-mode resonator is explained, the performance of the broadband BPF with the quadruple-mode resonator is simulated and optimized by HFSS. Finally, one broadband BPF prototype is fabricated for experimental verification of the predicted results. The substrate is RT/Duroid 5880 with a thickness of 0.508 mm, permittivity of 2.2 and loss tangent 0.0009.

## 2. PROPOSED TRIPLE-MODE OPEN IMPEDANCE-STEPPED STUB LOADED RESONATOR

As a starting part of this work, a novel resonator configured by adding two identical impedance-stepped open stubs denoted by length ( $b$ ,  $l_2$ ) and width ( $a$ ,  $w_1$ ) to a microstrip transmission line with length of  $2l_1 + 2m$  and widths of  $w$  is shown in Figure 1 and at first discussed. Since the resonator is symmetrical to the P point, Voltage (current) basically vanishes in the  $T$ - $T'$  plane when the wide  $w$  is very small, leading to the approximate transmission line circuit models represented in Figures 2(a) and (b). So the odd-even-mode method is implemented [4], and  $Y_{inodd} = 0$  and  $Y_{ineven} = 0$  give rise to the

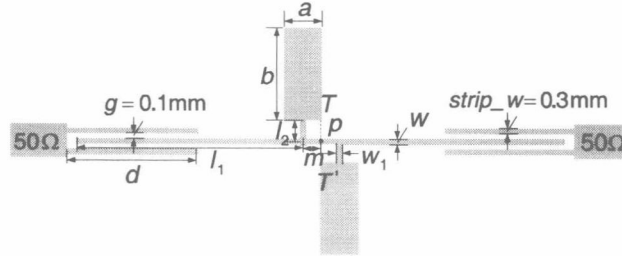


**Figure 1.** Schematic of the proposed triple-mode open impedance-stepped stub loaded resonator under the couple case.

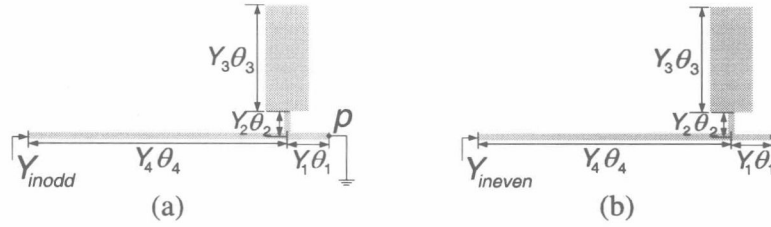


**Figure 2.** (a) Odd-mode equivalent circuit, and (b) even-mode equivalent circuit.

conditions for the odd mode resonator and even mode resonator in Figure 2(a) and Figure 2(b) (Herein, we choose  $w = w_1 = 0.3 \text{ mm}$ ):

$$(\tan \theta_1 \tan \theta_4 - 1)(Y_1 - Y_2 \tan \theta_2 \tan \theta_3) + Y_1 \tan \theta_2 + Y_2 \tan \theta_3 = 0 \quad (1)$$

$$(\tan \theta_1 + \tan \theta_4)(Y_1 - Y_2 \tan \theta_3 \tan \theta_2) + Y_2 \tan \theta_3 + Y_1 \tan \theta_2 = 0 \quad (2)$$

where  $\theta_1, \theta_2, \theta_3, \theta_4$  refer to the electrical lengths of the sections of lengths  $m, l_2, b$  and  $l_1$ , respectively. And  $Y_1$  and  $Y_2$  refer to characteristic admittances of the widths  $w$  and  $a$ , respectively.

We may choose the parameters of the impedance-stepped open stub:  $a = 2 \text{ mm}$ ,  $b = 5 \text{ mm}$ ,  $l_2 = 1 \text{ mm}$ ,  $w_1 = 0.3 \text{ mm}$ . Under the total parameters  $l_1 + m = 12.7 \text{ mm}$  keeping unchanged, resonant-mode frequencies varied  $m$  from the formulas (1) and (2) are interpreted in Figure 3. It can be seen that there are two odd modes and one even mode in the range of 0.1–7 GHz and the length  $m$  can adjust the locations of three resonant modes. When the impedance-stepped open stub moves near the center plane, it basically has no impact on the odd mode frequency  $f_{m1}$ . So, the  $f_{m1}$  is approximately determined by the following expression:

$$f_{m1} = \frac{c}{4(l_1 + m)\sqrt{\epsilon_{eff}}} \quad (3)$$

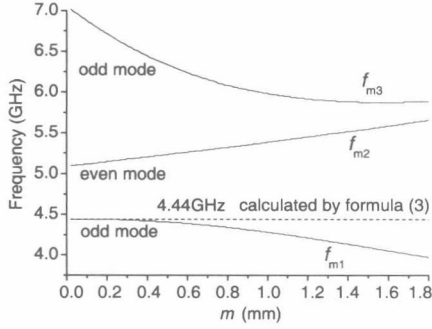


**Figure 3.** Resonant-mode frequencies with varied  $m$ .

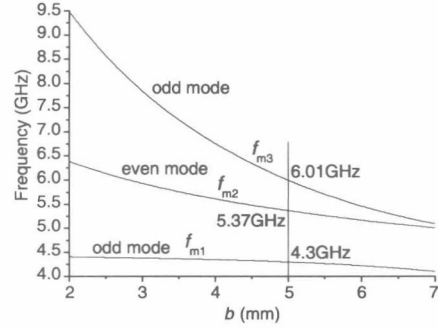


**Figure 4.** Resonant-mode frequencies with varied  $b$ .

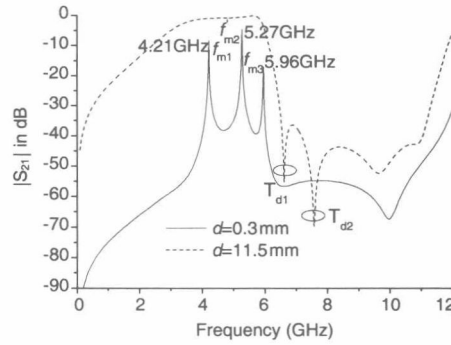


**Figure 5.** Simulated  $|S_{21}|$  in dB of weak and tight coupling triple-mode resonator.

where  $c$  is the speed of light and  $\varepsilon_{eff}$  is equivalent dielectric constant.

Furthermore, the specific effect of the length  $b$  on the resonant-mode frequencies is investigated and shown in Figure 4, where  $m$  is equal to 0.95 mm. As the length  $b$  varies from 2 mm to 7 mm, the resonant frequencies ( $f_{m2}$ ,  $f_{m3}$ ) tend to shift downwards and the resonant frequency ( $f_{m1}$ ) remains stationary. Thus,  $f_{m1}$  can be allocated in the lower cut-off frequency by reasonably choosing  $l_1$  and  $m$ , and the other two resonant frequencies can be adjusted within the desired passband by simply varying the parameter  $b$ .

The triple-mode resonator coupled to  $50\Omega$  input/output interdigital feeding lines under the selected coupling lengths of  $d = 0.3$  mm (the weak coupling case) and  $d = 11.5$  mm (the tight coupling case) [8] is simulated by HFSS and shown in Figure 5, where  $b = 5$  mm,  $g = 0.1$  mm, strip\_w=0.3 mm. Under the weak coupling case, the

first three simulated resonant-mode frequencies,  $f_{m1} = 4.21$  GHz,  $f_{m2} = 5.27$  GHz and  $f_{m3} = 5.96$  GHz, can work together to make up the desired passband. Under tight coupling case, two transmission zeros  $T_{d1}$  and  $T_{d2}$  near the upper cut-off frequency are shown in Figure 5 and separately generated by the identical impedance-stepped open stubs and the interdigital feeding lines [7], leading to a high upper rejection skirt. However, there is a poor rejection skirt in lower cut-off frequency.

### 3. QUADRUPLE-MODE STUB-LOADED RESONATOR AND BPF

Figure 6 illustrates the schematic of the proposed quadruple-mode stub-loaded resonator. Two identical short-circuited stubs with length  $l_3$  and width  $w_1$  are placed against the impedance-stepped open stubs in the triple-mode resonator. They are utilized to push the fourth resonant mode into the desired passband [10]. The fourth resonant frequency  $f_{m4}$  is approximately expressed by:

$$f_{m4} = \frac{c}{4(l_1 + l_3)\sqrt{\varepsilon_{eff}}} \quad (4)$$

Under the weak coupling case, the simulated  $|S_{21}|$  in dB of the quadruple-mode resonator for different values of  $l_3$  is interpreted in Figure 7. It is found that the resonant frequencies  $f_{m1}$ ,  $f_{m2}$  and  $f_{m3}$  are less affected by  $l_3$ , when it is changed from 1 to 3 mm. Hence, the fourth resonant frequency ( $f_{m4}$ ) moves up and works together with the three resonant frequencies ( $f_{m1}$ ,  $f_{m2}$ ,  $f_{m3}$ ) to form a novel quadruple-mode broadband BPF under the tight coupling case. Figure 9(a) interprets the simulated  $|S_{21}|$  in dB of the BPF and four resonant frequencies are in the passband (where  $l_3 = 3.1$  mm,  $d = 11.5$  mm). Compared

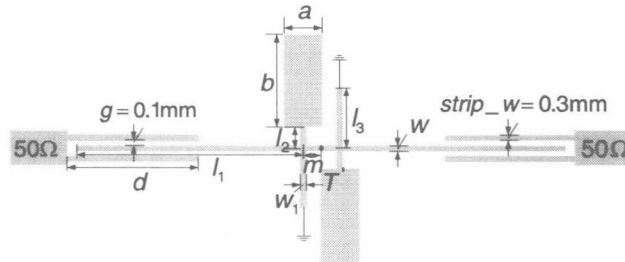


**Figure 6.** Schematic of the quadruple-mode stub-loaded resonator under the couple case.

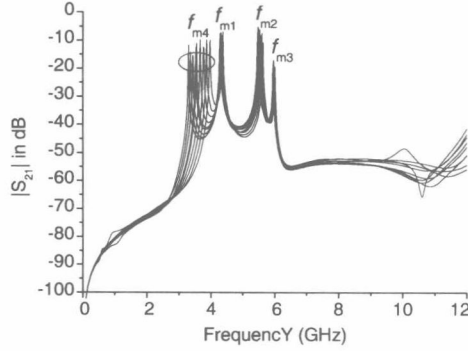


**Figure 7.** Simulated  $|S_{21}|$  in dB of weak coupling quadruple-mode stub-loaded resonator varied with  $l_3$ .



**Figure 8.** Photograph of the fabricated quadruple-mode BPF.

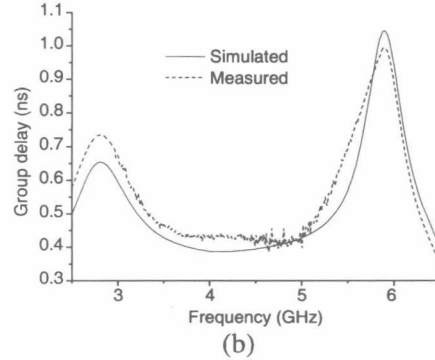
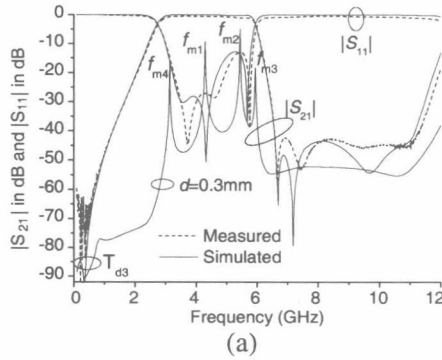


**Figure 9.** Simulated and measured frequency responses of the quadruple-mode broadband BPF. (a)  $|S_{21}|$  in dB and  $|S_{11}|$  in dB. (b) Group delay.

to the result in Figure 5, this quadruple-mode broadband BPF has enlarged attenuation skirt near the lower cut-off frequency attribute to the transmission zero  $T_{d3}$  created by the short-circuited stubs [10], in addition to keeping its high upper rejection skirt and wide upper-stopband performance.

After studying the characteristics of the quadruple-mode broadband BPF, the filter is fabricated on the RT/Duroid 5880 substrate, and its photograph is shown in Figure 8. The filtering performance is measured by Agilent network analyzer N5230A. The measured  $|S_{11}|$  in dB and  $|S_{21}|$  in dB as well as group delay are shown



in Figure 9 and illustrated good agreement with simulated results. The measured 2 dB passband is in the range of 2.96 to 5.81 GHz and its measured input return loss ( $|S_{11}|$  in dB) is less than  $-12.5$  dB. The upper-stopband in experiment is extended up to 11.5 GHz with an insertion loss better than  $-30$  dB. In addition, the measured in-band group delay is varying from 0.4 to 0.9 ns, which is quite small and flat in all the passband.

#### 4. CONCLUSION

In this letter, a novel compact triple-mode impedance-stepped stub loaded resonator is first studied and designed. The filter with the resonator under the tight coupling case has high upper rejection skirt and wide upper-stopband performance. After that, a quadruple-mode resonator is constituted by introducing two short-circuited stubs to the initial triple-mode resonator. Based on the resonator, a broadband BPF with the fractional bandwidth 65% is designed to exhibit its attractive sharp rejection skirts and wide upper-stopband. A filter prototype is fabricated to demonstrate the predicted performances in experiment.

#### REFERENCES

1. Tan, B. T., J. J. Yu, S. T. Chew, M.-S. Leong, and B.-L. Ooi, "A miniaturized dual-mode ring bandpass filter with a new perturbation," *IEEE Microwave and Wireless Components Lett.*, Vol. 53, No. 1, 343–345, Jan. 2005.
2. Huang, X. D. and C. H. Cheng, "A novel coplanar-waveguide bandpass filter using a dual-mode square-ring resonator," *IEEE Microwave and Wireless Components Lett.*, Vol. 16, No. 1, 13–15, Jan. 2006.
3. Kang, W., W. Hong, and J. Y. Zhou, "Performance improvement and size reduction of microstrip dual-mode bandpass filter," *Electronics Letter*, Vol. 44, No. 6, 421–422, Mar. 2008.
4. Hong, J.-S., H. Shaman, and Y.-H. Chun, "Dual-mode microstrip open-loop resonators and filters," *IEEE Transactions on Microwave Theory and Techniques*, Vol. 55, No. 8, 1764–1770, Aug. 2007.
5. Zhou, M., X. Tang, and F. Xiao, "Miniature microstrip bandpass filter using resonator-embedded dual-mode resonator based on source-load coupling," *IEEE Microwave and Wireless Components Lett.*, Vol. 20, No. 3, 139–141, Mar. 2010.

6. Shen, W., X.-W. Sun, and W.-Y. Yin, "A novel microstrip filter using three-mode stepped impedance resonator (TSIR)," *IEEE Microw. Wireless Compon. Lett.*, Vol. 19, No. 12, 774–776, Dec. 2009.
7. Lei, R. and L. Zhu, "Compact UWB bandpass filter using stub-loaded multiple-mode resonator," *IEEE Microw. Wireless Compon. Lett.*, Vol. 17, No. 1, 40–42, Nov. 2007.
8. Wong, S. W. and L. Zhu, "EBG-embedded multiple-mode resonator for UWB bandpass filter with improved upper-stopband performance," *IEEE Microw. Wireless Compon. Lett.*, Vol. 17, No. 6, 421–423, Jun. 2007.
9. Han, L., K. Wu, and X. P. Chen, "Compact ultra-wideband bandpass filter using stub-loaded resonator," *Electronics Letter*, Vol. 45, No. 10, May 2009.
10. Wong, S. W. and L. Zhu, "Quadruple-mode UWB bandpass filter with improved out-of-band rejection," *IEEE Microw. Wireless Compon. Lett.*, Vol. 19, No. 3, 152–154, Mar. 2009.
11. Ma, K., K. C. B. Liang, R. M. Jayasuriya, and K. S. Yeo, "A wideband and high rejection multimode bandpass filter using stub perturbation," *IEEE Microw. Wireless Compon. Lett.*, Vol. 19, No. 1, 24–26, Jan. 2009.

## HIGH SELECTIVITY BROADBAND BANDPASS FILTER WITH DUAL-MODE FOLDED-T-TYPE RESONATOR

H.-W. Deng, Y.-J. Zhao, X.-S. Zhang, W. Chen, and W. Liu

College of Information Science and Technology  
Nanjing University of Aeronautics and Astronautics  
Nanjing 210016, China

**Abstract**—In this letter, a compact and high selectivity broadband bandpass filter (BPF) is proposed using the dual-mode folded-T-type resonator and the short stub loaded parallel-coupling feed structure. The resonator can generate one even-mode and one odd-mode in the desired band. Two resonant frequencies can be adjusted easily to satisfy the bandwidth of the BPF. A parallel-coupling feed structure with a cross coupling has been applied to generate two transmission zeros in the lower and upper stopband. Furthermore, the loaded short stub can create two transmission zeros near the upper cut-off frequency and in the upper stopband. Simultaneity, the transmission zero in the lower stopband moves towards the cut-off frequency. One filter prototype with the fractional bandwidth 57% is fabricated for experimental verification of the predicted results. The size for the resonator is only  $0.156\lambda_g \times 0.303\lambda_g$  in which  $\lambda_g$  is the guided wavelength of 50  $\Omega$  microstrip at the center frequency.

### 1. INTRODUCTION

Broadband BPFs with compact size and high performance are highly demanded in many wireless communication systems [1]. The planar microstrip BPF has attractive features such as easier design, easier manufacture, lower cost, smaller size and lower radiation loss. In the past, a variety of microstrip planar broadband BPFs with improved electrical and/or geometrical features has been investigated [2–12]. Dual-mode resonators are attractive because the number of resonators required for a given degree of the filter is reduced by half, resulting in a compact filter configuration [3]. As is well known, the dual-mode

planar microstrip resonators are introduced for designing a compact filters [3–12]. Several types of dual-mode resonators with perturbation element have been investigated, including EBG-based resonator [4], ring resonator [5], square-ring resonator [6], multi-arc resonators [7]. Subsequently, the dual-mode resonators whose odd- and even-modes do not couple have been given in [8]. The open stubs can suppress the high harmonic resonant modes; therefore, a compact BPF using the open stub loaded dual-mode resonator in [9, 10] is presented with wide upper stopband performance. Nevertheless, the lower stopband suppression is as important as the higher one. A dual-mode open loop resonator with perturbation element in [11] is applied to design a compact filter with two transmission zeros on each side of the passband and the filter exhibits a desirable stopband response where the first spurious passband naturally occurs at  $3f_0$ . Furthermore, a broadband BPF with the fractional bandwidth 45% in [12] is designed with a dual-mode resonator composed of single stub at the center plane and two sections of transmission lines. However, the selectivity of the filter needs to be improved.

In this letter, a compact and high selectivity broadband BPF with the fractional bandwidth 57%, as shown in Figure 1, is proposed using the dual-mode folded-T-type resonator and the short stub loaded parallel-coupling feed structure. The even-mode resonant frequency can be flexibly controlled by the middle microstrip line, whereas the odd-mode one is fixed. Four transmission zeros are generated near the cut-off frequencies and in the stopband by the short stub loaded parallel-coupling feed structure. The good agreement between the simulated and measured results demonstrates our proposed structure.

## 2. DUAL-MODE BROADBAND FILTER

As shown in Figure 1, The dual-mode folded-T-type resonator formed by two microstrip lines is very compact in size, due to the folded

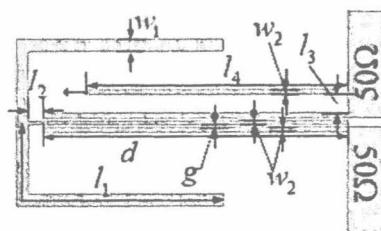


Figure 1. Schematic of the dual-mode broadband filter.